

Charged pion production from Au + Au collisions at $\sqrt{s_{NN}} = 2.4$ GeV in the Relativistic Vlasov-Uehling-Uhlenbeck model

Kyle Godbey*

Cyclotron Institute, Texas A&M University, College Station, TX 77843, USA[†]

Zhen Zhang[‡]

Sino-French Institute of Nuclear Engineering and Technology, Sun Yat-sen University, Zhuhai 519082, China

Jeremy W. Holt[§] and Che Ming Ko[¶]

Cyclotron Institute and Department of Physics and Astronomy,
Texas A&M University, College Station, TX 77843, USA

(Dated: July 29, 2021)

Using the isospin-dependent relativistic Vlasov-Uehling-Uhlenbeck (RVUU) model, we study charged pion (π^\pm) production in Au+Au collisions at $\sqrt{s_{NN}} = 2.4$ GeV. By fitting the density dependence of the Δ resonance production cross section in nuclear medium to reproduce the experimental π^\pm multiplicities, we obtain a good description of the rapidity distributions and transverse momentum spectra of π^\pm in collisions at various centralities. Some shortcomings in the description of π^+ production may indicate the need for including the strong potential on π^\pm in RVUU, which is at present absent. Predictions on the centrality dependence of proton rapidity distribution and transverse momentum spectrum are also presented.

I. INTRODUCTION

The study of pion production in heavy ion collisions has a long history as it is the lightest hadron that is produced in these collisions. From studies based on the Boltzmann-Uehling-Uhlenbeck (BUU) transport model [1], it was found that the inclusion of an equation of state (EOS) through the mean-field potentials acting on nucleons was essential to describe the pion yield produced in heavy ion collisions [2]. Unfortunately, the difference between the pion yields from the use of a soft and a stiff EOS is not large, making it difficult to extract from experimental pion data the information on the stiffness of nuclear EOS. Also, very different results on the pion yield as well as the pion rapidity distribution and transverse momentum spectrum are predicted from various transport models based on the BUU or the quantum molecular dynamics (QMD) approach [3].

More recently, the study of the π^-/π^+ yield ratio in heavy ion collisions at energies near the pion production threshold has drawn great attentions [4–15] as it was suggested in Ref. [16] that the stiffness of nuclear symmetry energy $E_{\text{sym}}(\rho)$ at high densities could have appreciable effect on this ratio. In this case, studying pion production in heavy ion collisions can greatly impact the progress of nuclear physics because the nuclear symmetry energy is at the heart of a complete understanding of

nuclear physics on various scales – governing the detail and structure of static nuclei [17–19], transfer and equilibration in low-energy nuclear reactions [20–23], and the structure and dynamics of neutron stars [24–27]. Despite this outsized impact on a wide range of physical phenomena, the high-density behavior of $E_{\text{sym}}(\rho)$ has not been as well constrained as other properties of nuclear matter (see [21] for a comprehensive review).

In heavy-ion collisions at beam energy E/A below 1.3 GeV, pions are produced from the decay of Δ resonances formed from NN inelastic scattering in the high density regions during the collision. As the $nn \rightarrow p\Delta^-$ and $pp \rightarrow n\Delta^{++}$ channels dominate the final charged pion multiplicities, the ratio of charged pions can provide insight into the isospin asymmetry of the dense matter in which they are formed. However, studies using various transport model studies were able to describe the pion data measured by the FOPI Collaboration [28] with nuclear symmetry energy at high densities ranging from super soft [4, 6] to stiff ones [5, 9]. This has led to the transport model evaluation project (TMEP) to understand the origin for the different predictions from a large number of transport models [29–31]. Some of these transport models have recently also been used to predict the charged pion multiplicities for reactions between neutron-rich Sn isotopes at beam energy of 270 AMeV, and none of them can describe the available data from the S π RIT Collaboration [32]. Although a subsequent study of the S π RIT pion data based on the dcQMD model [33] has put a constraint on the density slope of the nuclear symmetry energy at normal saturation density [34], the large uncertainty in the extracted value indicates the need for a better understanding and modeling of pion production in nuclear collisions.

Recently, charged pions produced from Au+Au collisions at beam energy of 1.23 AGeV or center of mass

*godbeyky@msu.edu

[‡]zhangzh275@mail.sysu.edu.cn

[§]holt@comp.tamu.edu

[¶]ko@comp.tamu.edu

[†]Current address: Facility for Rare Isotope Beams, Michigan State University, East Lansing, Michigan 48824, USA

energy $\sqrt{s_{NN}} = 2.4$ GeV have been measured by the HADES Collaboration [35]. Although the collision energy in this reaction is too high for the nuclear symmetry energy to affect the charged pion ratio, it adds to the available experimental data to benchmark model calculations and improve theoretical descriptions of pion production in heavy-ion collisions. Indeed, predicted pion yields from the five transport models used in studying the HADES pion data not only fail to describe the data but also disagree among themselves [36–40]. To find the possible reasons for the failure of these transport models, the current work builds upon recent extensions to the relativistic Vlasov-Uehling-Uhlenbeck (RVUU) model [10, 41] in an attempt to better describe π^\pm production in this reaction.

The structure of the paper is as follows: Sec. II exhibits an overview of the RVUU model and how it is used to determine pion production, along with the modifications to the in-medium density dependence of the $N + N$ inelastic cross section introduced in the current work. Sec. III then presents the results from RVUU simulations in comparison with experimental data from Ref. [35]. Finally, Sec. IV summarizes the results and discusses future directions.

II. RELATIVISTIC VLASOV-UHRLING-UHLENBECK MODEL

In the present study, we use the relativistic Vlasov-Uehling-Uhlenbeck (RVUU) model to further probe in-medium effects in heavy-ion collisions. The RVUU model describes the time evolution of the nucleonic phase-space distribution function, $f(\mathbf{r}, \mathbf{p}, t)$, by using the following transport equation,

$$\partial_t f + \mathbf{v} \cdot \nabla_{\mathbf{r}} f - \nabla_{\mathbf{r}} H \cdot \nabla_{\mathbf{p}} f = I_c, \quad (1)$$

In the above, H is the mean-field Hamiltonian of a nucleon, which was originally based on relativistic energy functionals including only isoscalar scalar σ and vector ω meson fields [42, 43], and has been later extended to also include the isovector scalar δ and vector ρ fields [41]. The resulting mean-field Hamiltonian [41] in Eq. (1) is then given by

$$H = \sqrt{m_N^{*2} + \mathbf{p}^{*2}} + g_\omega \omega^0 \pm g_\rho \rho_3^0, \quad (2)$$

for protons (+) and neutrons (−) of in-medium mass $m_N^* = m_N - (g_\sigma \sigma \pm g_\delta \delta_3)$ and kinetic momentum $\mathbf{p}^* = \mathbf{p} + g_\omega \boldsymbol{\omega} \pm g_\rho \boldsymbol{\rho}_3$ in the center-of mass frame of the colliding nuclei. The meson fields σ , δ_3 , ω^μ and ρ_3^μ in above equations are related to the proton and neutron scalar densities and their currents. Assuming the same interactions of the Δ resonance, whose isospin is three halves, with the σ and ω fields as those for nucleons and relating its interactions with the δ and ρ fields to those of nucleons via its isospin structure, the RVUU model has also been used to describe the evolution of the Δ resonances

in heavy ion collisions. For the values of the coupling constants g_σ , g_ω , g_δ and g_ρ as well as the nonlinear coupling constants of the scalar fields, we take the NL ρ parameter set given in Ref. [44], which can well reproduce our empirical knowledge on asymmetric nuclear matter.

The collision integral, I_c , in Eq. (1) describes the effect of nucleon-nucleon elastic and inelastic scatterings on the momenta of scattering nucleons and their probabilities to change to the Δ resonance. Governing the collision integral is thus the baryon-baryon elastic and inelastic cross sections. For the elastic scattering, the RVUU neglects its isospin dependence in the NN channels and assumes that the elastic scatterings in the $N\Delta$ and $\Delta\Delta$ channels have the same cross section as that in the NN channel. The total and differential baryon-baryon cross sections are then taken to have the following forms given in Ref. [45],

$$\sigma_{BB \rightarrow BB}^{\text{elastic}}(\text{mb}) = \begin{cases} 55, & \sqrt{s} < \sqrt{s_{\text{th}}} + 0.0213 \\ 20 + \frac{35}{1+100(\sqrt{s}-\sqrt{s_{\text{th}}}-0.0213)}, & \sqrt{s} \geq \sqrt{s_{\text{th}}} + 0.0213 \end{cases} \quad (3)$$

and

$$\frac{d\sigma_{BB \rightarrow BB}^{\text{elastic}}}{dt} \sim \exp(bt), \quad (4)$$

with

$$b = \exp \left[\frac{6\{3.65(\sqrt{s} - \sqrt{s_{\text{th}}} + 0.012)\}^6}{1 + \{3.65(\sqrt{s} - \sqrt{s_{\text{th}}} + 0.012)\}^6} \right]. \quad (5)$$

In the above, $s = (p_1 + p_2)^2$ with $p_i = (E_i, \mathbf{p}_i)$, where E_i denotes the energy of nucleon i and has the same expression as Eq.(2), is the square of the in-medium total center of mass energy of the scattering baryons and $\sqrt{s_{\text{th}}}$ is the minimum in-medium invariant mass of the final two baryons [41]. The variable $t = -2\mathbf{p}_{\text{c.m.}}^*(1 - \cos\theta)$ denotes the four momentum transfer, with $\mathbf{p}_{\text{c.m.}}^*$ and θ being, respectively, the kinetic momentum and scattering angle of one of the baryons in their center-of-mass frame.

For Δ resonance production in a nucleon-nucleon scattering, the RVUU uses the total and differential cross sections calculated in the one-boson exchange model and parametrized as a function of $d(\text{GeV}) = \sqrt{s} - \sqrt{s_{\text{th}}}$ for the reactions $p + p \rightarrow n + \Delta^{++}$ and $n + n \rightarrow p + \Delta^-$ [46], i.e.,

$$\sigma_{NN \rightarrow N\Delta}(\text{mb}) = \begin{cases} 1341d^{2.819}, & 0 \leq d \leq 0.186, \\ 18.51 - 235.2(d - 0.356)^2, & 0.186 < d \leq 0.436, \\ 1581(d + 2.014)^{-4.957}, & 0.436 < d \leq 2.486, \end{cases}$$

and

$$\frac{d\sigma_{NN \rightarrow N\Delta}}{d \cos \theta} \propto \begin{cases} \exp(b \cos \theta), & \text{forward,} \\ \exp(-b \cos \theta), & \text{backward,} \end{cases} \quad (6)$$

with

$$b = \begin{cases} 19.71d^{1.551}, & 0 \leq d \leq 0.416, \\ 33.41 \arctan[0.5404(d - 0.132)^{0.9784}], & 0.416 < d \leq 2.486. \end{cases}$$

A factor of $1/3$ is, however, multiplied to above $\sigma_{NN \rightarrow N\Delta}$ for the reactions $p + p \rightarrow p + \Delta^+$, $n + n \rightarrow n + \Delta^0$, $p + n \rightarrow p + \Delta^0$, and $p + n \rightarrow n + \Delta^+$ to take into account the isospin dependence of the $NN \rightarrow N\Delta$ reaction.

The threshold effects on Δ production cross section are taken into account as in Ref. [41]. The mass of the produced Δ resonance is determined according to

$$P(m^*) = \frac{\mathcal{A}(m^*)p^*}{\int_{m_{\min}^*}^{m_{\max}^*} dm^* \mathcal{A}(m^*)p^*(m^*)}, \quad (7)$$

where m^* is the effective mass of Δ , and m_{\min}^* and m_{\max}^* are the minimum and maximum effective masses of Δ that are allowed to form. The $\mathcal{A}(m^*)$ is the in-medium spectral function given by

$$\mathcal{A}(m^*) = \frac{1}{\mathcal{N}} \frac{4m_0^{*2}\Gamma}{(m^{*2} - m_0^{*2})^2 + m_0^{*2}\Gamma^2}, \quad (8)$$

with \mathcal{N} being the normalization factor and m_0^* being the Δ pole mass of 1.232 GeV shifted by the scalar potential. The total decay width of a Δ of effective mass m^* and isospin state m_T in its rest frame is taken to be

$$\Gamma = \sum_{m_t} \frac{0.47Cq^3}{m_\pi^2 + 0.6q^2}, \quad (9)$$

where m_t is the isospin state of the emitted pion, $C = |\langle \frac{3}{2}, m_T | 1, m_t, \frac{1}{2}, m_T - m_t \rangle|^2$ is the square of the Clebsch-Gordan coefficient from the isospin coupling. The magnitude of the momentum of the pion or nucleon in the Δ rest frame is denoted by q , and it is given by

$$q = \frac{\sqrt{[m^{*2} - (m_N^* + m_\pi)^2][m^{*2} - (m_N^* - m_\pi)^2]}}{2m^*}, \quad (10)$$

Note that in the calculation of Δ decay width and spectral function, we only include the effect of the scalar potential and neglect the vector potential for simplicity. For the reciprocal channel, $N + \Delta \rightarrow N + N$, its cross section is obtained by employing the detailed balance relation discussed in detail in Ref. [10].

The final mechanism to consider is the decay of Δ resonances into $N\pi$ pairs and its inverse, $N + \pi \rightarrow \Delta$. The pions produced by Δ decay are propagated in time as free particles unless they scatter with nucleons to again form Δ resonances. The N - π inelastic scattering cross section is related to the decay width of the formed Δ resonance via the detailed balance relation [10]. This naturally leads to a balance of Δ resonances and pions during the course of the reaction, with the sum of the two species being essentially constant after the period of highest density has passed. Fig. 1 shows this balance as a function of time, representing the sum of π^- , π^0 , and π^+ particles as π and the sum of Δ^- , Δ^0 , Δ^+ , and Δ^{++} resonances as Δ .

With this description alone a reasonable result is obtained for both the dynamics and total particle production in nuclear reactions. However, a density-dependent

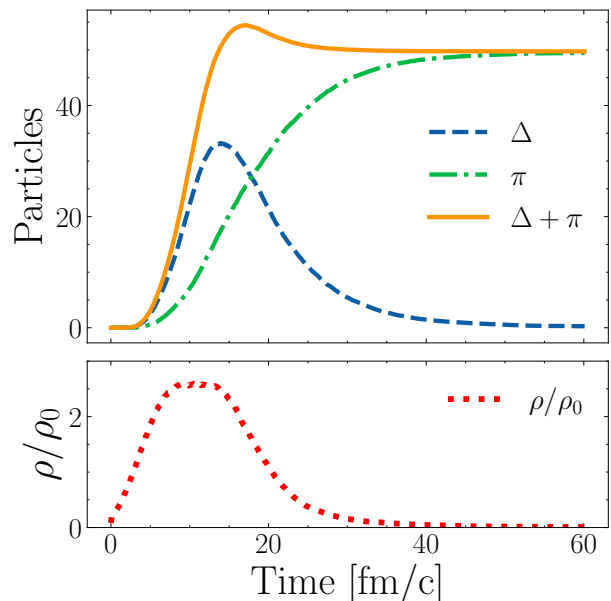


FIG. 1: (Color Online). Top panel: number of pions (dot-dashed lines) and Deltas (dashed lines) produced during a characteristic RVUU simulation of central Au+Au collisions at $\sqrt{s_{NN}} = 2.4$ GeV over time. The solid line corresponds to the sum of Deltas and pions. Bottom panel: maximal density in the central cells of the system at time t .

modification to the $\sigma_{NN \rightarrow N\Delta}$ cross sections are typically made to approximate the effects of the medium on Δ resonance production [47–49]. To extend this, the current work considers a modified scheme wherein the Δ^+ and Δ^{++} channels are allowed to have a slightly different density dependence than that of the Δ^0 and Δ^- channels. The modification of the $\sigma_{NN \rightarrow N\Delta}$ cross sections then takes the following form,

$$\sigma_{NN \rightarrow N\Delta}(\rho) = \sigma_{NN \rightarrow N\Delta} e^{-\alpha^\pm (\rho/\rho_0)^{3/2}}, \quad (11)$$

where α^+ corresponds to the constant factor to be used for Δ^+ and Δ^{++} production and α^- is to be used for the Δ^0 and Δ^- channels. α^\pm is then determined by a fit to experimental charged pion multiplicities. This decoupling of the two classes of delta production has the advantage of also allowing for more flexibility in the subsequent decays to π^- and π^+ , leading to a more robust fit to the experimental data without any major modification to the existing dynamics.

Upon performing the fitting procedure to the charged pion multiplicities reported in Ref. [35] for Au+Au collisions at $E_{\text{beam}} = 1.23$ A GeV or $\sqrt{s_{NN}} = 2.4$ GeV, values of $\alpha^+ = 0.36$ and $\alpha^- = 0.62$ were found. The smaller α^+ value found in the fit serves to slightly enhance the π^+ production when compared to π^- .

III. RESULTS

With the modified in-medium cross sections, $\sigma_{NN \rightarrow N\Delta}$, we now examine the predictions from the altered RVUU model.

A. Pions

TABLE I: Predicted multiplicities from the modified RVUU model and experimental results from Ref. [35]. Multiplicities are cited for the entire 0% – 40% centrality window.

	$M(\pi^-)$	$M(\pi^+)$
HADES	$11.1 \pm 0.6 \pm 0.6$	$6.0 \pm 0.3 \pm 0.3$
RVUU	11.26	6.12

First, in Table I, pion multiplicities over the full 0% – 40% centrality window are compared to those reported in Ref. [35]. The total number of both species of charged pions produced in the model compares well with the experimental values over the full range, indicating reasonable bulk pion production given the smaller suppression in the Δ^+ and Δ^{++} channels than Δ^- and Δ^0 channels

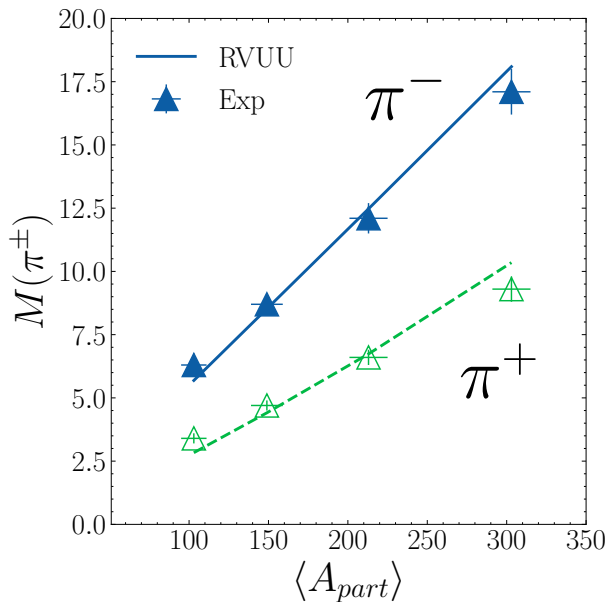


FIG. 2: (Color Online). Charged pion multiplicities from RVUU (lines) and experimental data (triangles) from Ref. [35]. Results are shown as a function of the mean number of participants, defined in Ref. [50]. Solid lines and filled symbols (dashed lines and empty symbols) correspond to π^- (π^+).

To examine the scaling with the mean number of participants, $\langle A_{part} \rangle$, we plot in Fig 2 the π^\pm multiplicities within four centrality bins of 0% – 10%, 10% – 20%,

20% – 30% and 30% – 40%, corresponding to the impact parameter (b) ranges of (0.0-4.7) fm, (4.7-6.6) fm, (6.6-8.1) fm, and (8.1-9.3) fm, respectively. In practice, the centrality determination and subsequent mapping of impact parameter ranges to $\langle A_{part} \rangle$ is performed in accordance with the values presented in [50]. The modification to pion production applies evenly across the range of centralities, with the behavior being roughly linear within the available range. In comparison to the experimental data, the model predictions follow closely for each of the centrality bins, with π^+ production at more peripheral and central collisions exhibiting a larger variance.

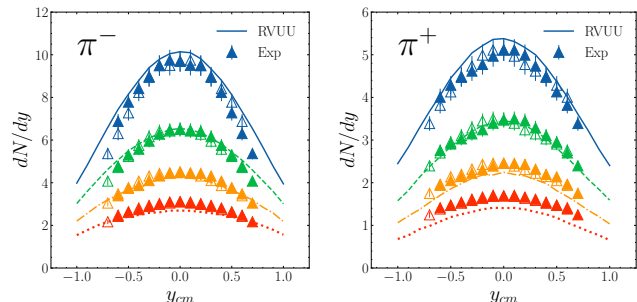


FIG. 3: (Color Online). Rapidity distributions of π^- (left window) and π^+ (right window) from RVUU (lines) and experimental data (triangles) from Ref. [35]. Results are shown across 4 centrality bins: 0% – 10% (blue, solid line), 10% – 20% (green, dashed line), 20% – 30% (orange, dot-dashed line), 30% – 40% (red, dotted line).

The left window of Fig. 3 shows rapidity distributions for negatively charged pions predicted by the RVUU model and the experimental data over the four centrality bins reported in Refs. [35, 50]. In this case, the model reproduces the experimental data well across all centralities despite being fitted to the total π^- multiplicity from all these classes of collisions. The results for π^+ , however, exhibit significantly more variance as shown in the right window of Fig. 3. Here it is seen that, at high centrality, pions are underproduced across all rapidities, while they are slightly overproduced at low centrality. This behavior reflects the small variance in π^+ multiplicity presented in Fig. 2 and is unlikely to be resolved by modifications to the in-medium cross sections alone. Indeed, the fitting procedure described in Sec. II could be performed anew for the peripheral or central collisions separately, though this would do nothing but shift the trend the other direction. Regardless, despite the suppression in total π^+ multiplicities at high centralities and their enhancement at low centralities, RVUU reproduces the approximate shape of the distribution as in the π^- case, indicating a reasonable description of π^+ dynamics.

Turning now to the transverse momentum p_t spectrum of π^\pm , Fig. 4 presents the model predictions along with the experimental data. The trend from the rapidity distributions continues, with the π^- results closely tracking the experimental data across the entire range of p_t bins. The π^+ results again deviate from the experimen-

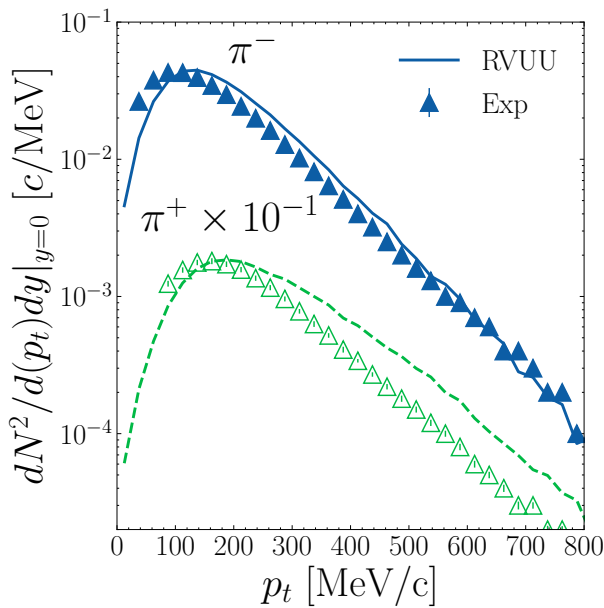


FIG. 4: (Color Online). Charged pion transverse momentum spectrum from RVUU (lines) and experimental data (triangles) from Ref. [35]. Negative pions are represented by filled blue symbols and solid blue line, while positive pions are scaled down by 10^{-1} and are drawn with hollow green symbols and green dashed line. Results are shown for mid-rapidity events for the most central (0% – 10%) class of collisions.

tal trend, exhibiting a different slope in the tail of the p_t distribution. Both results from RVUU show an overall shift of approximately 25 MeV from the peaks of the distributions. This deviation could be due to the absence of the pion mean-field potential, which is more attractive for π^+ than for π^- in neutron-rich nuclear matter[9, 10].

B. Protons

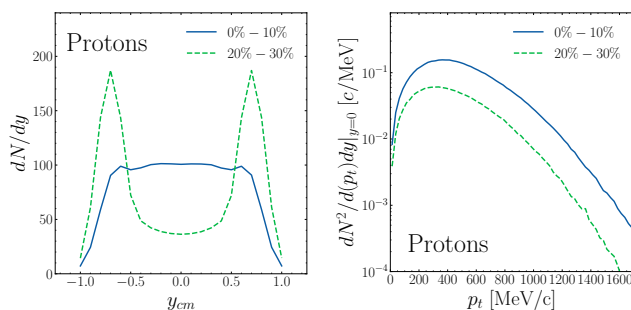


FIG. 5: (Color Online). Proton rapidity distributions (left window) and transverse momentum spectra (right window) for RVUU (lines) at two centrality classes, 0% – 10% (blue, solid line) and 20% – 30% (green, dashed line).

We have also studied the rapidity distribution and p_t spectrum of protons from Au+Au collision at $\sqrt{s_{NN}} =$

2.4 GeV. The predicted results are shown in Fig. 5 for the two centrality bins of 0-10% and 20-30%. As seen from the left window, the proton rapidity distribution changes from a shape with double peaks at the projectile and target rapidities to a flat one when the collision centrality increases, resulting in a stronger stopping of the colliding nucleons. For the proton p_t spectrum shown in the right window, it has a thermal-like spectrum with an effective temperature $T = 108$ MeV. A comparison of the predicted results with experimental data will be very useful to check if the in-medium nucleon-nucleon elastic cross section used in RVUU can properly describe the dynamics of nuclear collisions at this energy.

IV. CONCLUSIONS

In the present study, we have used the isospin-dependent RVUU model to study the production of charged pions from Au+Au collisions at $\sqrt{s_{NN}} = 2.4$ GeV. With the medium dependence of the Δ resonance production cross section from the nucleon-nucleon inelastic scattering determined by fitting the total multiplicities of π^- and π^+ measured in the HADES experiment, we have obtained a good description of the rapidity distributions of both π^- and π^+ for various centrality bins. For the π^- transverse momentum spectrum, a good description is also obtained. The predicted π^+ transverse momentum spectrum shows, however, too large an inverse slope parameter compared with the HADES data. We have attributed this discrepancy to the absence of the pion mean-field potential in the RVUU model. The reasonable success of the RVUU model in describing the HADES pion data is in contrast to the results from other transport models [36–40] used by the HADES Collaboration to compare with its data, which all overestimate the π^- and π^+ multiplicities by about a factor of two. The reason for the difference between our results and those from other transport models are mainly due to our introduction of a density-dependent reduction factor to the nucleon-nucleon inelastic cross section, which is absent in other models. To understand the origin of this reduction factor requires further theoretical studies. Using the extended RVUU model, we have also made predictions on the rapidity distribution and transverse momentum spectrum of protons from the same nuclear collision. A strong dependence of the proton stopping on the centrality of the collision is predicted, which provides a useful observable to constrain the medium dependence of the nucleon-nucleon elastic cross section once the experimental data on protons becomes available for comparison with our predictions.

Acknowledgments

This work was supported in part by the U.S. Department of Energy under Award Nos. DE-SC0015266

(C.M.K.) and DE-SC0013365 (K.G.), the Welch Foundation under Grant No. A-1358 (K.G. and C.M.K.), the National Natural Science Foundation of China under Grant No. 11905302 (Z.Z.), and the National Science Foundation under Grant No. PHY1652199 and by the U.S. Department of Energy National Nuclear Security

Administration under Grant No. DE-NA0003841 (J.W.H.). K.G. acknowledges partial support through computational resources and services provided by the Institute for Cyber-Enabled Research at Michigan State University.

-
- [1] G. F. Bertsch and S. Das Gupta, *Phys. Rept.* **160**, 189 (1988).
- [2] H. Kruse, B. V. Jacak, and H. Stoecker, *Phys. Rev. Lett.* **54**, 289 (1985).
- [3] E. E. Kolomeitsev et al., *J. Phys. G* **31**, S741 (2005), nucl-th/0412037.
- [4] Z. Xiao, B. A. Li, L. W. Chen, G. C. Yong, and M. Zhang, *Phys. Rev. Lett.* **102**, 062502 (2009).
- [5] Z. Q. Feng and G. M. Jin, *Phys. Lett. B* **683**, 140 (2010).
- [6] W. J. Xie, J. Su, L. Zhu, and F. S. Zhang, *Phys. Lett. B* **718**, 1510 (2013).
- [7] J. Xu, C. M. Ko, and Y. Oh, *Phys. Rev. C* **81**, 024910 (2010).
- [8] J. Xu, L. W. Chen, C. M. Ko, B. A. Li, and Y. G. Ma, *Phys. Rev. C* **87**, 067601 (2013).
- [9] M. D. Cozma, *Phys. Rev. C* **95**, 014601 (2017).
- [10] Z. Zhang and C. M. Ko, *Phys. Rev. C* **95**, 064604 (2017), URL <https://link.aps.org/doi/10.1103/PhysRevC.95.064604>.
- [11] B. A. Li, *Phys. Rev. C* **92**, 034603 (2015).
- [12] G. Ferini, M. Colonna, T. Gaitanos, and M. Di Toro, *Nucl. Phys. A* **762**, 147 (2005).
- [13] T. Song and C. M. Ko, *Phys. Rev. C* **91**, 014901 (2015).
- [14] G.-C. Yong, *Phys. Rev. C* **96**, 044605 (2017).
- [15] N. Ikeno, A. Ono, Y. Nara, and A. Ohnishi, *Phys. Rev. C* **93**, 044612 (2016).
- [16] B.-A. Li, *Phys. Rev. Lett.* **88**, 192701 (2002), URL <https://link.aps.org/doi/10.1103/PhysRevLett.88.192701>.
- [17] X. Viñas, M. Centelles, X. Roca-Maza, and M. Warda, *The European Physical Journal A* **50**, 27 (2014), ISSN 1434-601X, URL <https://doi.org/10.1140/epja/i2014-14027-8>.
- [18] M. Baldo and G. Burgio, *Progress in Particle and Nuclear Physics* **91**, 203 (2016), ISSN 0146-6410, URL <https://www.sciencedirect.com/science/article/pii/S0146641016300254>.
- [19] D. Adhikari, H. Albatineh, D. Androic, K. Aniol, D. S. Armstrong, T. Averett, S. Barcus, V. Bellini, R. S. Beniniwatha, J. F. Benesch, et al. (2021), 2102.10767.
- [20] V. Baran, M. Colonna, V. Greco, and M. Di Toro, *Physics Reports* **410**, 335 (2005), ISSN 0370-1573, URL <https://www.sciencedirect.com/science/article/pii/S0370157305000025>.
- [21] B.-A. Li, L.-W. Chen, and C. M. Ko, *Physics Reports* **464**, 113 (2008), ISSN 0370-1573, URL <https://www.sciencedirect.com/science/article/pii/S0370157308001269>.
- [22] K. Godbey, A. S. Umar, and C. Simenel, *Phys. Rev. C* **95**, 011601(R) (2017).
- [23] C. Simenel, K. Godbey, and A. S. Umar, *Phys. Rev. Lett.* **124**, 212504 (2020), URL <https://link.aps.org/doi/10.1103/PhysRevLett.124.212504>.
- [24] J. M. Lattimer and M. Prakash, *Science* **304**, 536 (2004), ISSN 0036-8075, <https://science.sciencemag.org/content/304/5670/536.full.pdf>, URL <https://science.sciencemag.org/content/304/5670/536>.
- [25] A. Steiner, M. Prakash, J. Lattimer, and P. Ellis, *Physics Reports* **411**, 325 (2005), ISSN 0370-1573, URL <https://www.sciencedirect.com/science/article/pii/S0370157305001043>.
- [26] J. M. Lattimer and M. Prakash, *Physics Reports* **442**, 109 (2007), ISSN 0370-1573, the Hans Bethe Centennial Volume 1906-2006, URL <https://www.sciencedirect.com/science/article/pii/S0370157307000452>.
- [27] B.-A. Li, P. G. Krastev, D.-H. Wen, and N.-B. Zhang, *The European Physical Journal A* **55**, 117 (2019), ISSN 1434-601X, URL <https://doi.org/10.1140/epja/i2019-12780-8>.
- [28] W. Reisdorf et al. (FOPI), *Nucl. Phys. A* **781**, 459 (2007), nucl-ex/0610025.
- [29] J. Xu et al., *Phys. Rev. C* **93**, 044609 (2016), 1603.08149.
- [30] Y.-X. Zhang et al., *Phys. Rev. C* **97**, 034625 (2018), 1711.05950.
- [31] A. Ono et al., *Phys. Rev. C* **100**, 044617 (2019), 1904.02888.
- [32] G. Jhang et al. (S π RIT, TMEP), *Phys. Lett. B* **813**, 136016 (2021), 2012.06976.
- [33] M. D. Cozma and M. B. Tsang (2021), 2101.08679.
- [34] J. Estee et al. (S π RIT), *Phys. Rev. Lett.* **126**, 162701 (2021), 2103.06861.
- [35] J. Adamczewski-Musch, O. Arnold, C. Behnke, A. Belounnas, A. Belyaev, J. C. Berger-Chen, A. Blanco, C. Blume, M. Böhmer, P. Bordalo, et al., *The European Physical Journal A* **56**, 259 (2020), ISSN 1434-601X, URL <https://doi.org/10.1140/epja/s10050-020-00237-2>.
- [36] C. Hartnack, R. K. Puri, J. Aichelin, J. Konopka, S. A. Bass, H. Stoecker, and W. Greiner, *Eur. Phys. J. A* **1**, 151 (1998), nucl-th/9811015.
- [37] W. Cassing and E. L. Bratkovskaya, *Phys. Rept.* **308**, 65 (1999).
- [38] J. Aichelin, E. Bratkovskaya, A. Le Fèvre, V. Kireyeu, V. Kolesnikov, Y. Leifels, V. Voronyuk, and G. Coci, *Phys. Rev. C* **101**, 044905 (2020), 1907.03860.
- [39] O. Buss, T. Gaitanos, K. Gallmeister, H. van Hees, M. Kaskulov, O. Lalakulich, A. B. Larionov, T. Leitner, J. Weil, and U. Mosel, *Phys. Rept.* **512**, 1 (2012), 1106.1344.
- [40] H. Petersen, D. Oliinychenko, M. Mayer, J. Staudenmaier, and S. Ryu, *Nucl. Phys. A* **982**, 399 (2019), 1808.06832.
- [41] T. Song and C. M. Ko, *Phys. Rev. C* **91**, 014901 (2015), URL <https://link.aps.org/doi/10.1103/PhysRevC.91.014901>.

- [42] C. M. Ko, Q. Li, and R. Wang, Phys. Rev. Lett. **59**, 1084 (1987), URL <https://link.aps.org/doi/10.1103/PhysRevLett.59.1084>.
- [43] C. M. Ko and Q. Li, Phys. Rev. C **37**, 2270 (1988), URL <https://link.aps.org/doi/10.1103/PhysRevC.37.2270>.
- [44] B. Liu, V. Greco, V. Baran, M. Colonna, and M. Di Toro, Phys. Rev. C **65**, 045201 (2002), URL <https://link.aps.org/doi/10.1103/PhysRevC.65.045201>.
- [45] G. Bertsch and S. Das Gupta, Physics Reports **160**, 189 (1988), ISSN 0370-1573, URL <https://www.sciencedirect.com/science/article/pii/0370157388901706>.
- [46] S. Huber and J. Aichelin, Nuclear Physics A **573**, 587 (1994), ISSN 0375-9474, URL <https://www.sciencedirect.com/science/article/pii/0375947494902321>.
- [47] A. Engel, W. Cassing, U. Mosel, M. Schäfer, and G. Wolf, Nuclear Physics A **572**, 657 (1994), ISSN 0375-9474, URL <https://www.sciencedirect.com/science/article/pii/0375947494904057>.
- [48] A. Larionov, W. Cassing, S. Leupold, and U. Mosel, Nuclear Physics A **696**, 747 (2001), ISSN 0375-9474, URL <https://www.sciencedirect.com/science/article/pii/S0375947401012167>.
- [49] A. B. Larionov, W. Cassing, M. Effenberger, and U. Mosel, The European Physical Journal A - Hadrons and Nuclei **7**, 507 (2000), ISSN 1434-601X, URL <https://doi.org/10.1007/PL00013652>.
- [50] J. Adamczewski-Musch, O. Arnold, C. Behnke, A. Belounnas, A. Belyaev, J. C. Berger-Chen, J. Biernat, A. Blanco, C. Blume, M. Böhmer, et al., The European Physical Journal A **54**, 85 (2018), ISSN 1434-601X, URL <https://doi.org/10.1140/epja/i2018-12513-7>.